

THE FAR-INFRARED SPECTRUM OF THE OH RADICAL¹

J. M. BROWN AND J. E. SCHUBERT

Department of Chemistry, Southampton University

K. M. EVENSON

National Bureau of Standards

AND

H. E. RADFORD

Harvard-Smithsonian Center for Astrophysics

Received 1982 January 4; accepted 1982 February 8

ABSTRACT

The frequencies, wavelengths, and line strengths for transitions between the lowest spin-rotation levels of the OH molecule have been calculated from the recently reported laser magnetic resonance spectra.

Subject headings: line identifications — molecular processes

Radioastronomy has demonstrated that the observation of atomic and molecular lines provides much useful information about the chemistry and the physics of the interstellar environment. It is likely that spectral lines in the far-infrared will be equally informative, perhaps even more so (Watson and Storey 1980). The first such observations, both in emission and absorption, have only recently been reported. For example, emissions by carbon atoms have been detected in several interstellar sources by Phillips *et al.* (1980), while strong absorption lines of the hydroxyl radical, OH, have been detected in the direction of Sgr B2 by Storey, Watson, and Townes (1981). By comparison with the microwave region, the far-infrared is largely unexplored. There is a pressing need for good laboratory data to aid searches and assignments of spectra from the interstellar clouds and nebulae. Such information may also be useful in other contexts, such as the modeling of population inversions (Destombes *et al.* 1977).

We have recently completed a study of the laser magnetic resonance (LMR) spectrum of the OH radical in its ground state at far-infrared wavelengths (Brown *et al.* 1981). In these experiments, a molecular transition frequency is tuned into coincidence with that of a fixed frequency laser by the application of a variable magnetic field (0–2 T). All the coincidences with known far-infrared laser lines have been studied and analysed, from an effective Hamiltonian given by Brown *et al.* (1978). Zero field frequencies are not measured directly in such experiments, but the quality of the fit of the

magnetic resonance data for OH is such that the extrapolation to zero field can be performed with some confidence. We have computed the frequencies of individual hyperfine transitions involving all rotational levels up to $J = 4\frac{1}{2}$. The results are given in Table 1 and are summarized in the diagram in Figure 1, which shows the low lying energy levels of OH. The frequencies of transitions between levels studied directly in the LMR spectrum are quite reliable; the standard deviation of a single observation in the fit to the LMR frequencies was 1.9 MHz and, allowing for some uncertainty in the model-dependent extrapolation to zero magnetic field, we estimate the uncertainty of the transition frequencies obtained in this way to be ± 3 MHz. The energy levels involved in the other transitions are extrapolated in J value, and consequently, the frequencies become progressively less reliable. The vacuum wavelengths and line strengths of the transitions are also given in Table 1. The line strength $S_{F'F''}$ can be used to assess the relative intensity of an individual transition. It is defined by

$$S_{F'F''} = \left| \langle \gamma' F' || \mathcal{D}_q^{(1)}(\omega)^* || \gamma'' F'' \rangle \right|^2, \quad (1)$$

where the quantity on the right-hand side is the reduced matrix element of the rotation matrix (Brink and Satchler 1968) and γ stands for subsidiary quantum numbers. The intensity of a line in absorption can be obtained by multiplying the line strength by the square of the dipole moment μ (1.6676 debye for OH, Meerts and Dymanus 1973) and by the population factor for the lower level. The Einstein A -coefficients for spontaneous emission

¹Work supported in part by NASA contract W-15, 047.

TABLE 1
CALCULATED SPIN-ROTATION TRANSITION FREQUENCIES
FOR THE OH RADICAL IN ITS GROUND STATE

$F'_i - F''_i$	Transition ^a $J' - J''$	$F' - F''$	Frequency (GHz)	Vacuum Wavelength (μm)	Line Strength ^b
$F_1 - F_1 \dots$	$2\frac{1}{2} - 1\frac{1}{2}$	$2^+ - 2^-$	2509.9337(30) ^c	119.4424	1.350×10^{-1}
		$2^+ - 1^-$	2509.9869(30)	119.4398	1.215
		$3^+ - 2^-$	2509.9477(30)	119.4417	1.889
		$2^- - 2^+$	2514.2971(30)	119.2351	1.349×10^{-1}
		$2^- - 1^+$	2514.3523(30)	119.2325	1.214
		$3^- - 2^+$	2514.3155(30)	119.2342	1.889
$F_1 - F_1 \dots$	$3\frac{1}{2} - 2\frac{1}{2}$	$3^- - 3^+$	3543.7887(30)	84.59659	1.204×10^{-1}
		$3^- - 2^+$	3543.8027(30)	84.59626	2.409
		$4^- - 3^+$	3543.7812(30)	84.59677	3.252
		$3^+ - 3^-$	3551.1882(30)	84.42032	1.204×10^{-1}
		$3^+ - 2^-$	3551.2066(30)	84.41989	2.409
		$4^+ - 3^-$	3551.1876(30)	84.42034	3.252
$F_1 - F_1 \dots$	$4\frac{1}{2} - 3\frac{1}{2}$ ^d	$4^+ - 4^-$	4592.515(>3)	65.27850	1.011×10^{-1}
		$4^+ - 3^-$	4592.507(>3)	65.27860	3.538
		$5^+ - 4^-$	4592.493(>3)	65.27880	4.448
		$4^- - 4^+$	4602.891(>3)	65.13134	1.011×10^{-1}
		$4^- - 3^+$	4602.890(>3)	65.13135	3.538
		$5^- - 4^+$	4602.879(>3)	65.13152	4.447
$F_2 - F_2 \dots$	$1\frac{1}{2} - 1\frac{1}{2}$	$1^- - 1^+$	1834.7347(30)	163.3983	3.232×10^{-1}
		$1^- - 0^+$	1834.7496(30)	163.3969	6.463×10^{-1}
		$2^- - 1^+$	1834.7466(30)	163.3972	1.616
		$1^+ - 1^-$	1837.7458(30)	163.1305	3.233×10^{-1}
		$1^+ - 0^-$	1837.8362(30)	163.1225	6.467×10^{-1}
		$2^+ - 1^-$	1837.8160(30)	163.1243	1.616
$F_2 - F_2 \dots$	$2\frac{1}{2} - 1\frac{1}{2}$ ^d	$2^+ - 2^-$	3036.260(>3)	98.73741	1.948×10^{-1}
		$2^+ - 1^-$	3036.272(>3)	98.73702	1.754
		$3^+ - 2^-$	3036.278(>3)	98.73683	2.728
		$2^- - 2^+$	3036.576(>3)	98.72714	1.949×10^{-1}
		$2^- - 1^+$	3036.646(>3)	98.72486	1.754
		$3^- - 2^+$	3036.647(>3)	98.72482	2.729
$F_2 - F_2 \dots$	$3\frac{1}{2} - 2\frac{1}{2}$ ^d	$3^+ - 3^-$	4209.566(>3)	71.21695	1.399×10^{-1}
		$3^+ - 2^-$	4209.638(>3)	71.21574	2.798
		$4^+ - 3^-$	4209.640(>3)	71.21570	3.778
		$3^- - 3^+$	4212.283(>3)	71.17102	1.399×10^{-1}
		$3^- - 2^+$	4212.300(>3)	71.17072	2.797
		$4^- - 3^+$	4212.306(>3)	71.17062	3.776
$F_2 - F_1 \dots$	$\frac{1}{2} - 1\frac{1}{2}$	$1^+ - 1^-$	3786.1853(30)	79.18061	1.017×10^{-2}
		$0^+ - 1^-$	3786.1704(30)	79.18092	2.034×10^{-2}
		$1^+ - 2^-$	3786.1322(30)	79.18172	5.085×10^{-2}
		$1^- - 1^+$	3789.2706(30)	79.11614	1.006×10^{-2}
		$0^- - 1^+$	3789.1802(30)	79.11803	2.012×10^{-2}
		$1^- - 2^+$	3789.2155(30)	79.11729	5.030×10^{-2}
$F_2 - F_1 \dots$	$1\frac{1}{2} - 1\frac{1}{2}$ ^d	$1^- - 1^+$	5619.255(>3)	53.35093	1.984×10^{-2}
		$2^- - 1^+$	5619.267(>3)	53.35082	3.968×10^{-3}
		$1^- - 2^-$	5619.200(>3)	53.35145	3.967×10^{-3}
		$2^- - 2^+$	5619.211(>3)	53.35134	3.571×10^{-2}
		$1^+ - 1^-$	5628.682(>3)	53.26157	1.940×10^{-2}
		$2^+ - 1^-$	5628.752(>3)	53.26091	3.878×10^{-3}
$F_2 - F_1 \dots$	$2\frac{1}{2} - 1\frac{1}{2}$ ^d	$1^+ - 2^-$	5628.629(>3)	53.26208	3.880×10^{-3}
		$2^+ - 2^-$	5628.699(>3)	53.62141	3.492×10^{-2}
		$2^+ - 2^-$	8657.139(>3)	34.62951	4.201×10^{-4}
		$2^+ - 1^-$	8657.192(>3)	34.62929	3.784×10^{-3}
		$3^+ - 2^-$	8657.157(>3)	34.62944	5.885×10^{-3}
		$2^- - 2^+$	8663.607(>3)	34.60365	4.080×10^{-4}
		$2^- - 1^+$	8663.663(>3)	34.60343	3.675×10^{-3}
		$3^- - 2^+$	8663.679(>3)	34.60337	5.716×10^{-3}

TABLE 1—Continued

$F'_i - F''_i$	Transition ^a $J' - J''$	$F' - F''$	Frequency (GHz)	Vacuum Wavelength (μm)	Line Strength ^b
$F_2 - F_1 \dots$	$1\frac{1}{2} - 2\frac{1}{2}$	$2^- - 2^+$	3110.9450(30)	96.36701	3.120×10^{-3}
		$1^- - 2^+$	3110.9332(30)	96.36737	2.807×10^{-2}
		$2^- - 3^+$	3110.9310(30)	96.36744	4.367×10^{-2}
		$2^+ - 2^-$	3112.7344(30)	96.31161	3.062×10^{-3}
		$1^+ - 2^-$	3112.6642(30)	96.31378	2.756×10^{-2}
		$2^+ - 3^-$	3112.7160(30)	96.31218	4.287×10^{-2}
$F_2 - F_1 \dots$	$2\frac{1}{2} - 2\frac{1}{2}$ ^d	$2^+ - 2^-$	6141.174(>3)	48.81680	3.548×10^{-2}
		$3^+ - 2^-$	6141.192(>3)	48.81665	2.535×10^{-3}
		$2^+ - 3^-$	6141.156(>3)	48.81694	2.535×10^{-3}
		$3^+ - 3^-$	6141.174(>3)	48.81680	5.069×10^{-2}
		$2^- - 2^+$	6155.341(>3)	48.70444	3.441×10^{-2}
		$3^- - 2^+$	6155.413(>3)	48.70388	2.456×10^{-3}
		$2^- - 3^+$	6155.327(>3)	48.70455	2.458×10^{-3}
		$3^- - 3^+$	6155.399(>3)	48.70399	4.917×10^{-2}
$F_2 - F_1 \dots$	$3\frac{1}{2} - 2\frac{1}{2}$ ^d	$3^+ - 3^-$	10358.930(>3)	28.94049	2.843×10^{-4}
		$3^+ - 2^-$	10358.948(>3)	28.94044	5.691×10^{-3}
		$4^+ - 3^-$	10359.004(>3)	28.94028	7.682×10^{-3}
		$3^- - 3^+$	10359.492(>3)	28.93892	2.937×10^{-4}
		$3^- - 2^+$	10359.506(>3)	28.93888	5.878×10^{-3}
		$4^- - 3^+$	10359.515(>3)	28.93885	7.935×10^{-3}
		$3^- - 3^+$	2598.175(>3)	115.3858	1.273×10^{-3}
		$2^- - 3^+$	2598.104(>3)	115.3889	2.547×10^{-2}
$F_2 - F_1 \dots$	$2\frac{1}{2} - 3\frac{1}{2}$ ^d	$3^- - 4^+$	2598.176(>3)	115.3857	3.438×10^{-2}
		$3^+ - 3^-$	2603.420(>3)	115.1533	1.303×10^{-3}
		$2^+ - 3^-$	2603.402(>3)	115.1541	2.605×10^{-2}
		$3^+ - 4^-$	2603.428(>3)	115.1530	3.517×10^{-2}
		$3^- - 3^+$	6802.268(>3)	44.07243	4.356×10^{-2}
		$4^- - 3^+$	6802.292(>3)	44.07227	1.614×10^{-3}
		$3^- - 4^+$	6802.269(>3)	44.07242	1.614×10^{-3}
		$4^- - 4^+$	6802.293(>3)	44.07227	5.647×10^{-2}
$F_2 - F_1 \dots$	$3\frac{1}{2} - 3\frac{1}{2}$ ^d	$3^+ - 3^-$	6821.176(>3)	43.95026	4.199×10^{-2}
		$4^+ - 3^-$	6821.250(>3)	43.94978	1.553×10^{-3}
		$3^+ - 4^-$	6821.183(>3)	43.95021	1.555×10^{-3}
		$4^+ - 4^-$	6821.257(>3)	43.94974	5.444×10^{-2}
		$4^+ - 4^-$	2204.925(>3)	135.9649	5.984×10^{-4}
		$3^+ - 4^-$	2204.851(>3)	135.9695	2.095×10^{-2}
		$4^+ - 5^-$	2204.938(>3)	135.9642	2.634×10^{-2}
		$4^- - 4^+$	2223.219(>3)	134.8461	6.136×10^{-4}
$F_2 - F_1 \dots$	$3\frac{1}{2} - 4\frac{1}{2}$ ^d	$3^- - 4^+$	2223.196(>3)	134.8475	2.147×10^{-2}
		$4^- - 5^+$	2223.247(>3)	134.8448	2.699×10^{-2}

^aQuantum numbers for the upper state are indicated by single primes and those for the lower state by double primes. The superscripts on the F quantum number values indicate the parity of the states involved in accordance with the definition in Brown *et al.* 1978.

^bFor definition, see eq. (1).

^cEstimated uncertainty in units of the last quoted decimal place.

^dTransition involves level(s) not studied directly in the LMR spectrum.

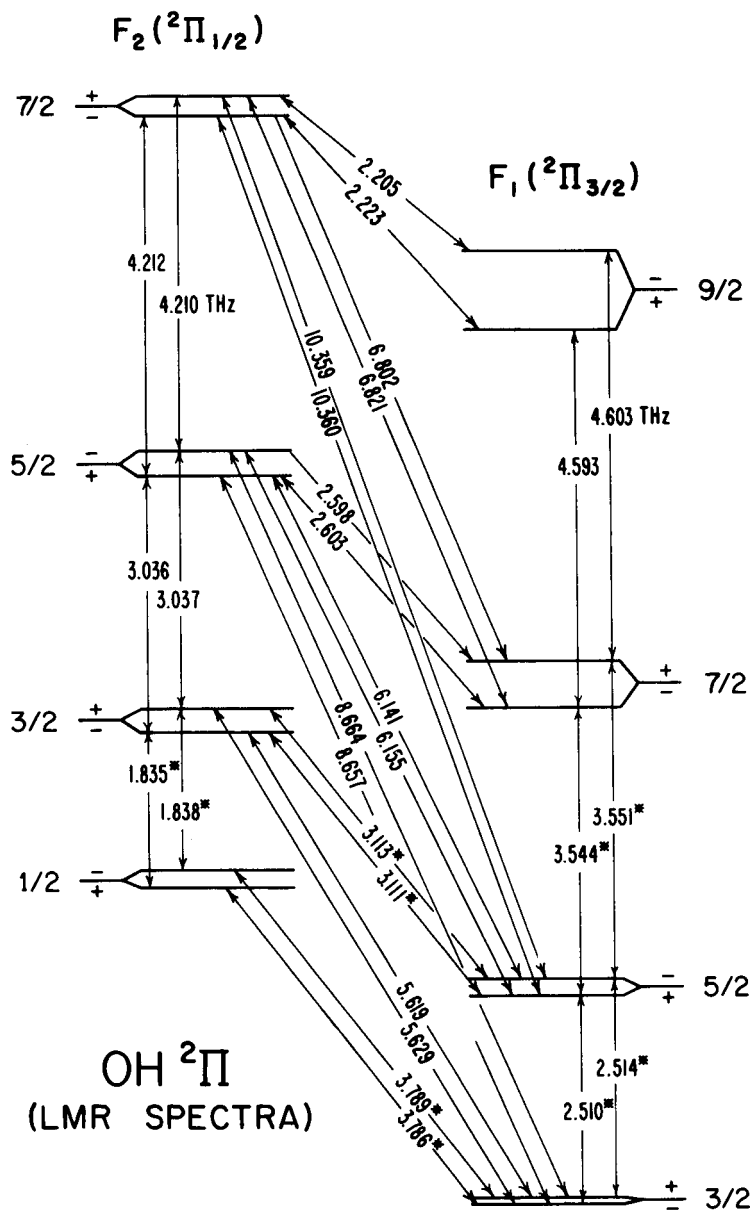


FIG. 1.—The low lying energy levels of the OH radical, connected by electric dipole transitions ($+ \leftrightarrow -$) in the far infrared. The parity doubling (or lambda doubling) has been exaggerated for the sake of clarity. The transition frequencies are given in THz.

from state i to j can be calculated from the line strengths in Table 1 by use of

$$A_{i \rightarrow j} = (16\pi^3 \nu_{ij}^3 / 3\epsilon_0 hc^3) (2F_i + 1)^{-1} S_{ij} \mu^2. \quad (2)$$

REFERENCES

- Brink, D. M., and Satchler, G. R. 1968, *Angular Momentum* (Oxford: Oxford University Press).
 Brown, J. M., Kaise, M., Kerr, C. M. L., and Milton, D. J. 1978, *Molec. Phys.*, **36**, 553.
 Brown, J. M., Kerr, C. M. L., Wayne, F. D., Evenson, K. M., and Radford, H. E. 1981, *J. Molec. Spectrosc.*, **86**, 544.
 Destombes, J. L., Marliere, C., Baudry, A., and Brillet, J. 1977, *Astr. Ap.*, **60**, 55.
 Meerts, W. L., and Dymanus, A. 1973, *Chem. Phys. Letters*, **23**, 45.
 Phillips, T. G., Huggins, P. J., Kuiper, T. B. H., and Miller, R. E. 1980, *Ap. J. (Letters)*, **238**, L103.
 Storey, J. W. V., Watson, D. M., and Townes, C. H. 1981, *Ap. J. (Letters)*, **244**, L27.
 Watson, D. M., and Storey, J. W. V. 1980, *Internat. J. Infrared and Millimetre Waves*, **1**, 609.

J. M. BROWN, K. M. EVENSON, H. E. RADFORD, and J. E. SCHUBERT: Laser Frequency Metrology Group, Time and Frequency Division, U. S. Department of Commerce, National Bureau of Standards, Boulder, CO 80303